

Recent Douglas-fir Mortality in the Klamath Mountains Ecoregion of Oregon: Evidence for a Decline Spiral

Max Bennett,^{1,*}  David C. Shaw,² and Laura Lowrey³

¹Forestry and Natural Resources Extension, Oregon State University, Southern Oregon Research & Extension Center, 569 Hanley Rd, Central Point, OR, 97502, USA (max.bennett@oregonstate.edu).

²Department of Forest Engineering, Resources, and Management, Oregon State University, 216 Peavy Forest Science Complex, 3100 SW Jefferson Way, Corvallis, OR 97331, USA (david.shaw@oregonstate.edu).

³USDA Forest Service, Forest Health Protection, Medford Interagency Office, 3040 Biddle Rd, Medford, OR, 97504, USA (laura.lowrey@usda.gov).

*Corresponding author email: max.bennett@oregonstate.edu

Abstract

Recent increases in Douglas-fir (*Psuedotsuga menziesii* var. *menziesii*) mortality in the Klamath Mountains ecoregion raise concerns about the long-term resilience of Douglas-fir in the ecoregion and increased potential for uncharacteristic wildfire. We used data from the USDA Forest Service Aerial Detection Survey and ninety-six field plots to explore the relationships between physiographic and climate variables and Douglas-fir mortality. Our results provide strong evidence for a decline spiral in which Douglas-fir growing on hot, dry sites (predisposing factor) are further stressed by drought (inciting factor) and are then exploited by the flatheaded fir borer (*Phaenops drummondii*) and other secondary biotic agents (contributing factors), resulting in decline and mortality. At the landscape scale, Douglas-fir mortality increased as average annual precipitation declined and average climatic water deficit increased. We developed a risk score integrating several environmental variables associated with drought and heat stress to predict the likelihood and intensity of mortality at the stand scale.

Study Implications: Douglas-fir mortality in the Klamath Mountains ecoregion commonly occurs during and following drought on hot, dry sites that are already climatically marginal for the species. Landowners and managers can use climatic water deficit to identify high mortality risk sites at the landscape scale and our risk score integrating topographic and site factors for risk assessment at the stand scale. Steering management toward oak-pine restoration may be warranted in high risk locations. Projections of future climatic water deficit suggest that the area of marginal, high risk habitat for Douglas-fir will increase substantially by 2055.

Keywords: Douglas-fir, *Psuedotsuga menziesii*, forest health, tree mortality, flatheaded fir borer, *Phaenops drummondii*, Klamath Mountains ecoregion, decline spiral, drought, Aerial Detection Survey

Coastal Douglas-fir (*Psuedotsuga menziesii* var. *menziesii*) is the dominant species in many low-to-mid-elevation dry forests in the Klamath Mountains ecoregion of southwestern Oregon and northern California (Franklin and Dyrness 1988). These forests provide essential ecosystem services ranging from wildlife habitat and carbon sequestration to timber production. However, recent increases in Douglas-fir (DF) mortality (Buhl et al. 2017; Schaupp 2017, figure 1) raise concerns about the long-term resilience of this species in the ecoregion, the loss of key ecosystem services, and the potential for increased fuel loading and uncharacteristic wildfire (Hessburg et al. 2019). At the same time, DF mortality on some sites, such as former oak woodlands, presents opportunities for restoration. The Klamath ecoregion is well known for its high topographic and edaphic variability (Vander Schaaf et al. 2004) and such variability can influence both tree growth (Hoyleman et al. 2018) and mortality (Bost et al. 2019; Paz-Kagan et al. 2017). A better understanding of the physiographic and climatic factors influencing DF mortality would help land managers predict when and where DF is

most vulnerable and prioritize stands for preventative thinning and restoration treatments.

Since the mid-1970s, the USDA Forest Service (Forest Service) Aerial Detection Survey (ADS) has attributed observed DF mortality in the Klamath ecoregion primarily to the flatheaded fir borer (FB) (*Phaenops drummondii*) (Coleoptera: Buprestidae), a wood borer, rather than the Douglas-fir beetle (DFB) (*Dendroctonus pseudotsugae*) (Coleoptera: Curculionidae). The FB is unusual in that unlike most native Buprestid beetles, it infests and often kills its live conifer host (Furniss and Carolin 1977; Schaupp and Strawn 2016). Although the FB is little studied, ADS data and field observations suggest that FB-related DF mortality typically occurs during and immediately after drought and in locations where Douglas-fir is near its lower threshold of water availability such as valley margins and the fringes of Oregon white oak stands (Goheen and Wilhite 2021; Oregon Department of Forestry 2016). Conversely, trees in lower slope positions, in stand interiors, and on deeper soils may be buffered from moisture stress and experience lower mortality rates from the FB and related agents.

Received: November 17, 2022. Accepted: February 14, 2023.

© The Author(s) 2023. Published by Oxford University Press on behalf of the Society of American Foresters. All rights reserved. For permissions, please e-mail: journals.permissions@oup.com.



Figure 1. Recent Douglas-fir mortality in the Klamath ecoregion. Top: Typical Douglas-fir mortality pattern, 2016 USDA Forest Service (USFS) and Oregon Department of Forestry (ODF) Aerial Detection Survey (B. Schroeder, USFS). Middle: Douglas-fir mortality, 2016, Applegate valley (B. Schaupp, USFS). Bottom: Douglas-fir mortality, 2022, Applegate valley (C. Adlam, Oregon State University). Note Proximity of Oregon white oak woodlands to dead Douglas-fir in middle and bottom images.

The FB is found throughout the western United States and Canada and colonizes true firs (*Abies*), western hemlock (*Tsuga heterophylla*), spruce (*Picea*), and larch (*Larix*) in addition to DF (Furniss and Carolin 1977; Gibson 2010). As landscapes become increasingly droughty with climate

change, the impacts of this insect on DF and perhaps other species will likely increase (Agne et al. 2018; Halofsky et al. 2022). Therefore, recent DF mortality patterns in the Klamath ecoregion may have implications for management of DF forests in a broader geographic area.

A landscape vegetation change context is important for understanding recent DF mortality in the Klamath ecoregion. Studies of fire history in the ecoregion suggest that prior to Euro-American settlement in the mid-19th century, fires were predominantly of low and mixed severity (Metlen et al. 2018 and references therein), supporting relatively open, spatially heterogeneous forests. Fire suppression since the early 1900s has resulted in fuels accumulation, increases in stand density, and a shift to higher proportions of more shade tolerant, less fire-resistant trees (Knight et al. 2020; Leonzo and Keyes 2010). Data on changes in species composition in the ecoregion are limited, but it is reasonable to infer that Douglas-fir has increased in abundance and has encroached on some sites, such as white oak woodlands, following fire exclusion (Hosten et al. 2007).

We use Mannion's "decline disease spiral" as a framework for hypothesizing the interaction of environmental variables that contribute to DF mortality in the Klamath ecoregion. This framework describes a process whereby predisposing, inciting, and contributing factors lead to progressive loss of tree vigor and eventual death (Mannion 1991). Specifically, DF trees growing on marginal, water-stressed sites (predisposing factors) are more vulnerable to episodic drought stress (inciting factors) that impairs their physiological functioning, making them more susceptible to FB and other biotic agents (contributing factors), resulting in tree decline and death (figure 2). Carbon starvation and hydraulic failure may occur as a precursor to these biotic agents or may be amplified by them (McDowell et al. 2008). Although most DF mortality in the ecoregion has been attributed to the FB in ADSs, the actual causes of mortality, as well as site factors, may be more complex and need validation by systematic field investigation.

Study Objectives

Our objectives were to (1) assess the relationships between environmental variables, including physiographic, edaphic, and stand characteristics, and the spatial and temporal patterns of recent (2000–2019) DF mortality in the Oregon portion of the Klamath ecoregion; (2) determine the likely causes of DF mortality in the study area and evaluate the relative contributions of the FB, other insect and disease agents, and abiotic damage, to the extent feasible; and (3) develop a risk score based on stand and environmental variables to predict the likelihood and intensity of mortality at the stand scale. Understanding the underlying patterns of tree mortality in the region will greatly improve future forest management.

Methods

Study Area

The study area encompassed the Oregon portion of the Klamath ecoregion and a part of the western Cascades ecoregion (figure 3) which, with the exception of a small area in the southern coast range, comprises the entire area in Oregon where the FB has been detected by the ADS. This mountainous region (elevation range 3–2,288 m) has a Mediterranean climate with cool, moist winters and hot, dry summers (Franklin and Dyrness 1988). Precipitation varies considerably and generally increases with elevation and proximity to the ocean (PRISM Climate Group, Oregon State University, 2022). Natural vegetation includes mixed conifer and mixed evergreen forests, oak woodlands, chaparral and other

non-conifer types (Franklin and Dyrness 1988). Douglas-fir is the most abundant tree species and a major constituent of most forest types. Other common tree species include ponderosa pine (*Pinus ponderosa*), sugar pine (*Pinus lambertiana*), white fir (*Abies concolor*), Oregon white oak (*Quercus garryana*), California black oak (*Quercus kelloggii*), and Pacific madrone (*Arbutus menziesii*).

Analysis of ADS Data in Relation to Climate and Historic Vegetation

We used mortality data from the ADS administered by the Forest Service and cooperating state partners to explore the relationships between Douglas-fir mortality, climate, and vegetation in the study area. The ADS program provides the most comprehensive, long-term dataset of forest mortality trends associated with insects and disease across the United States and can be used to describe the relative scope and scale of large-scale mortality events (Coleman et al. 2018). However, the accuracy of ADS estimates of trees per acre damaged or killed tends to decline in larger damage polygons (Coleman et al. 2018) and can also be affected by survey timing, surveyor experience, visibility, and other factors (Malesky et al. 2019).

Despite these limitations, the ADS is useful for assessing trends and comparing the relative magnitude of mortality associated with damaging agents across space and time. For this analysis we calculated the cumulative DF mortality (in trees per acre) for the period 2000–2019 that was attributed to the FB. Mortality was summed in 1 km grid cells to provide a trees killed per square kilometer metric, recognizing that this metric was likely inaccurate in an absolute sense but was valuable for relative comparisons across space (i.e., as a heat map of the intensity of mortality). To facilitate comparisons of areas with higher and lower levels of mortality, we classified the number of FB-killed trees per each 1-km grid cell as follows: no mortality, <2 trees killed/km², 2–20 trees killed/km², 20–100 trees killed/km², 100–500 trees killed/km², and >500 trees killed/km².

We used gridded climate data (800 m) from PRISM (PRISM Climate Group, Oregon State University, 2022) for mean annual precipitation, June–August maximum monthly temperature, and June–August maximum monthly vapor pressure deficit for the period 1990–2020 (i.e., climate "normals"). We obtained gridded (90 m) climate water deficit (CWD) data, an integrated measure of moisture stress that is calculated from the difference between actual evapotranspiration and potential evapotranspiration, based on precipitation, water storage in soils and snow, and solar radiation for 1980–2010 (Cansler et al. 2022). These gridded climate data were intersected with and averaged for each 1-km grid cell, allowing for comparisons of cumulative DF mortality, average climate, and CWD over a given time period. Mean elevation for each 1-km grid cell was calculated from a 30 m digital elevation model. We used gradient nearest neighbor (GNN) cover data (Landscape Ecology Modeling Mapping and Analysis 2014) to mask non-forest areas, defined as grid cells in which >50% of the cell had <10% forest cover. All spatial analyses were conducted using ArcMap 10.8.

We also compared year-to-year FB mortality with weather variables that might influence mortality levels using a time series of FB mortality, the number of trees killed each year across the entire study area from 1975–2019. We credited each year's mortality to the year prior to the year of detection in the aerial survey, on the assumption that most trees detected

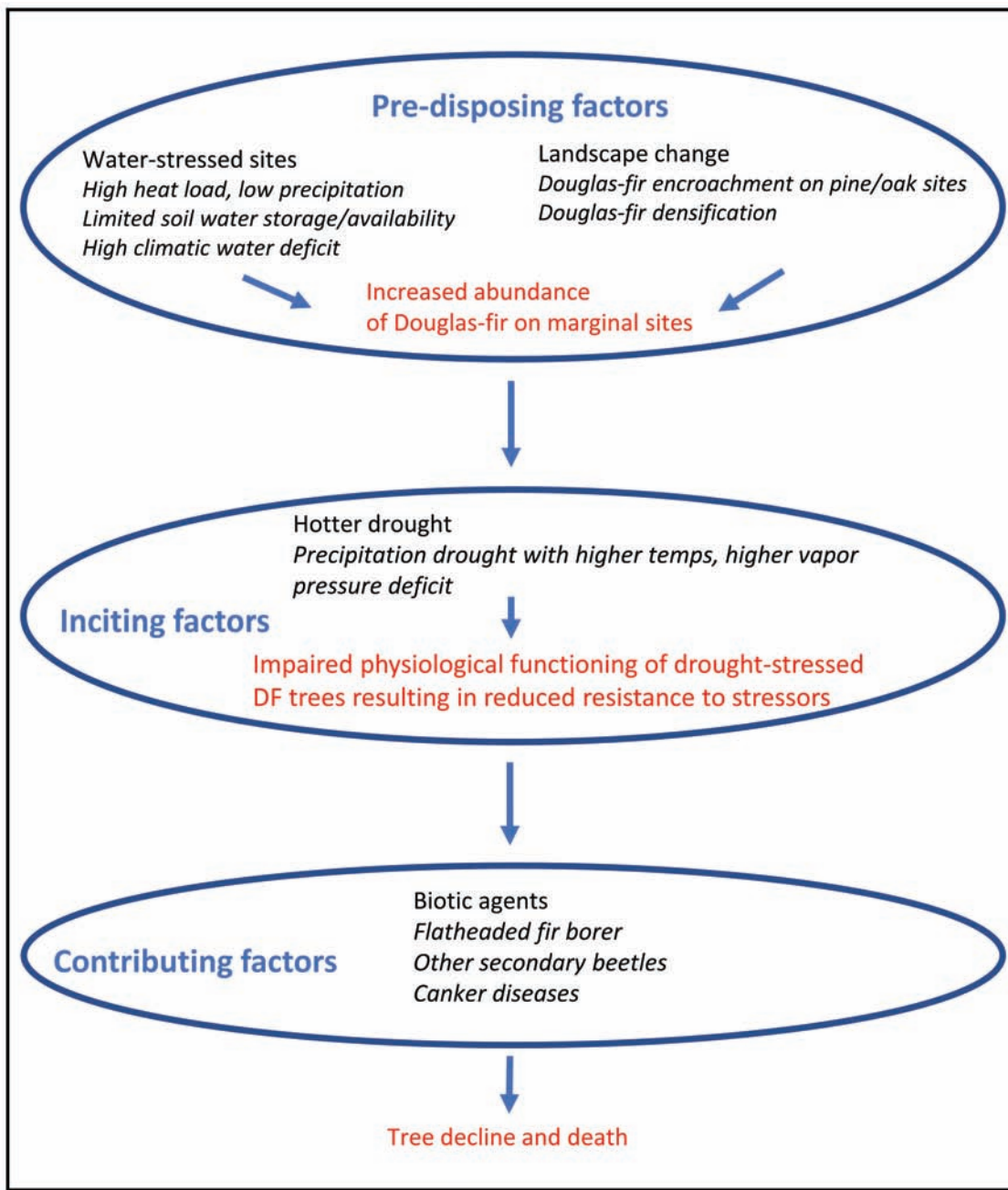


Figure 2. Hypothesized causes of Douglas-fir decline in Klamath ecoregion of Oregon. Douglas-fir trees growing on already marginal, water-stressed sites (predisposing factors) are vulnerable to episodic drought stress (inciting factors) that impairs their physiological functioning, making them more susceptible the flatheaded fir borer and other biotic agents (contributing factors), resulting in tree decline and death. Carbon starvation and hydraulic failure may occur as a precursor to these biotic agents or may be amplified by them.

during summer detection flights were likely killed in the year previous (Lowrey 2022, personal observation). Drought indices used were the Standardized Precipitation Index (SPI) and the Palmer Drought Severity Index (PDSI) (National Center for Atmospheric Research 2022). The SPI is a measure of precipitation anomaly over a defined time frame, with negative values representing drought. We compared mortality trends with 1-, 2-, and 5-year growing season SPI (April 1 through October 30). The PDSI accounts for precipitation and temperature, with negative values representing drought (National Center for Atmospheric Research 2022). We used annual and growing season PDSI. We also compared mortality to summer

maximum and minimum temperatures. Data for the weather variable time series were obtained from Climate Toolbox (<https://climatetoolbox.org/>) and averaged over all grid cells in the study area for the year or growing season.

For the comparison of historic vegetation and FB mortality, we used a historic vegetation layer representing dominant vegetation in the study area in 1938 that was created from General Land Office survey data and other historic maps (Tobalske 2002). Dominant vegetation in the historic map was classified in terms of broad types such as “Douglas-fir,” “Ponderosa pine” and “Oak savannah.” Although lacking in spatial precision and subject to the limitations of historical

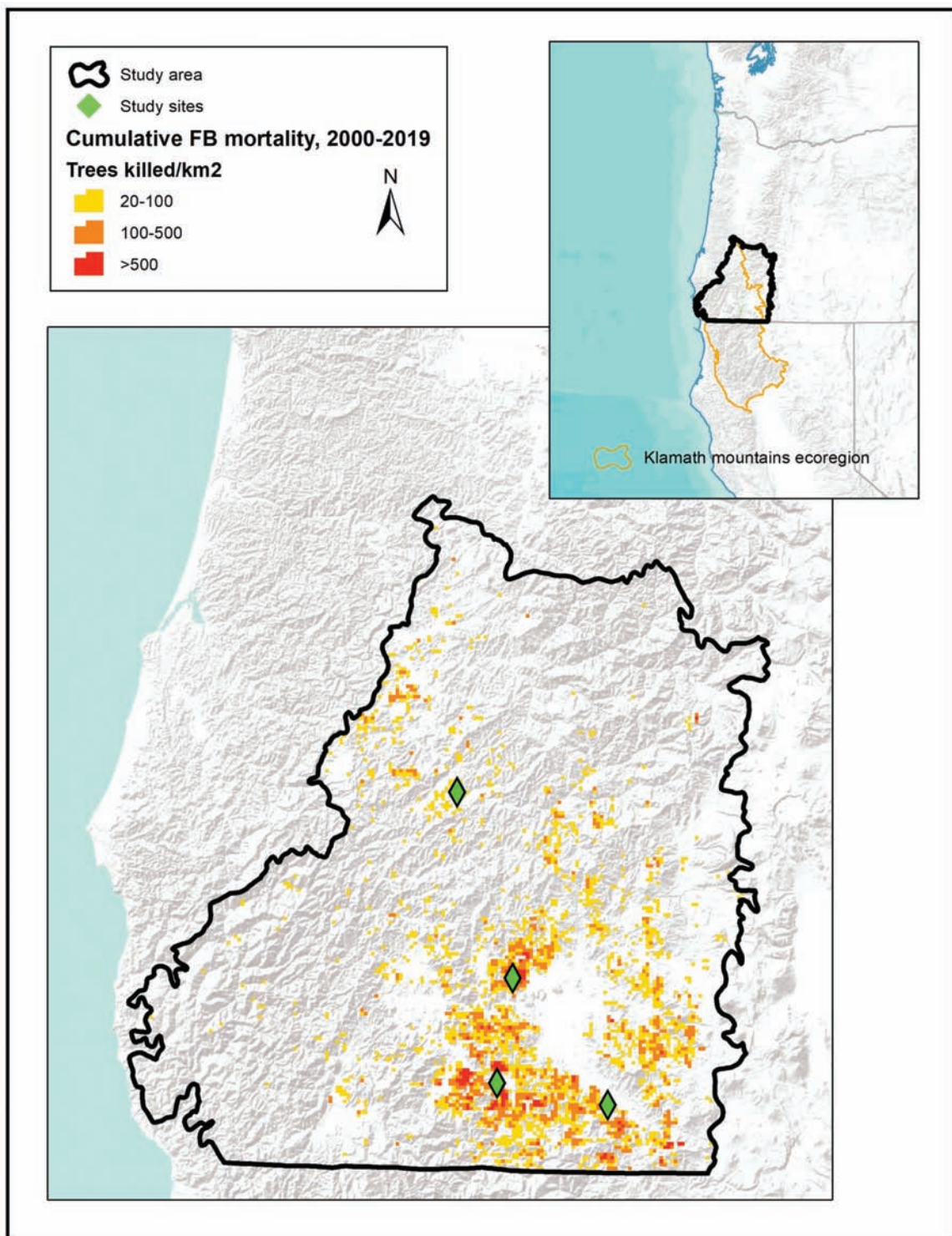


Figure 3. Relationship of study area and study sites to Klamath ecoregion. Cumulative Aerial Detection Survey 2000–2019 Douglas-fir mortality attributed to the flatheaded fir borer (FB) in the study area is shown, with mortality displayed in classes based on trees killed per square kilometer. Grid cells with <20 trees killed/km² are not shown.

data (Schulte and Mladenoff 2001), this dataset provides a reasonable approximation of regional vegetation types before the era of intensive logging and early in the era of fire exclusion. We intersected FB polygons from the period 2000–2018 with the historic vegetation polygons and then calculated the percentage of cumulative FB mortality for the period falling within each historic vegetation type.

Field Sampling and Data Collection

To assess patterns of DF mortality in relation to stand-scale topographic and site factors, we collected data from field plots distributed systematically across four study sites that were representative of low elevation forests in the study area with past and on-going DF mortality associated with the FB (figure 3). The study sites ranged from 64 to 272

ha (158–672 ac) in size and were located in four different 5th field watersheds. Each site was topographically complex and contained substantial recent and past DF mortality. Field plots consisted of two nested subplots, a 20 Basal Area Factor variable radius plot, and a 0.4 ha circular fixed area plot. The variable radius subplot (20 BAF) was used to determine the basal area of live, dead, and dying trees 20 cm (8 in) diameter at breast height (DBH) and larger, by species. We considered a DF tree to be dying if it had more than 50% recent foliage loss or branch dieback or signs and symptoms of FB or bark beetle attack (e.g., woodpecker “shaved” bark). We measured DBH and, in forty-five of the ninety-six total plots, estimated recent crown loss on every other DF in the plot up to a maximum of three trees. Crown loss ratings were categorized in 25% increments, with ratings from 0 (no crown loss) to 4 (75%–100% crown loss). Within the 0.4 ha fixed area subplot we determined the presence or absence of one or more Oregon white oak (*Quercus garryana*) trees of sapling size or larger and the

presence or absence of recent DF mortality in trees 20 cm (8 in) DBH and larger. We then obtained plot data for several environmental variables that we hypothesized were related to heat or moisture stress or both, based on the literature or on prior field observation, and would thus be potentially associated with and predictive of stand-level DF mortality. These included heat load index, climate water deficit, topographic position, and aspect. A description of all environmental variables and variable categories used with the plot data is included in [Table 1](#).

Field plots were located along a systematic grid within each site to effectively sample DF mortality in relation to topographic variation. Of the ninety-seven grid plots initially installed across all four sites, seventy-three (75%) had at least 4.6m²/ha (20 ft²/ac) of Douglas-fir basal area, and data from these plots were used for the subsequent analysis. Because this sampling frame might not adequately sample the typically patchy distribution of DF mortality across the sites, we also mapped and sampled DF mortality patches on each

Table 1. Description of environmental variables used with field plot data and percent of plots with and without Douglas-fir (DF) mortality for each variable. Continuous variables were binned based on breakpoints seen in the data to highlight differences in plot mortality status associated with higher and lower levels of the variable.

Variable	Description/expected relationship with DF mortality	Percent of plots		
		Variable category	With DF mortality	Without DF mortality
Quga	Oregon white oak (<i>Quercus garryana</i>) presence/absence from 1-ac subplot. Oregon white oak (WO) is an indicator of droughty soils (Hosten et al. 2007); prior field observation suggested WO presence is associated with DF mortality.	WO present	74%	26%
		WO absent	48%	52%
HLI	Heat load index at plot center. HLI is a measure of incident solar radiation based on aspect & slope derived from a digital elevation model, with values ranging from 0 to 1 (Buttrick et al. 2015). Expect positive correlation of HLI & mortality.	HLI>0.84	74%	26%
		HLI 0.61–0.84	62%	38%
		HLI<0.61	29%	71%
CWD	Climate water deficit (CWD, in mm) is an integrated measure of moisture stress calculated from the difference between actual evapotranspiration and potential evapotranspiration, based on input for precipitation, water storage in soils & snow, & solar radiation, for 1980–2010 (Cansler et al. 2022). Expect positive correlation of CWD & mortality.	CWD >375	87%	13%
		CWD 300–375	56%	44%
		CWD <300	22%	78%
Edge	Distance from plot center to stand edge (EDGE, in m). Stand edges often have higher temperatures and evaporative demand than stand interiors, leading to greater stress on trees. Prior field observation suggested that DF mortality was more common along stand edges than within stand interiors.	Distance to edge<10m	66%	34%
		Distance to edge>10m	53%	47%
TPI	Topographic position index (TPI) compares the elevation of a cell with the elevation of adjacent cells and is used to classify landforms from a digital elevation model (Jenness 2006). TPI was derived from a 10m digital elevation model based on a 500-meter neighborhood and classified into ridges/upper slope positions (TPI > 70) and otherwise (TPI<71). Expect higher DF mortality on upper slopes & ridges.	Ridges/upper slopes	74%	26%
		Other landforms	52%	48%
Aspect	Aspect at plot center, derived from a 10m digital elevation model, then classified into SW aspect/otherwise & NE aspect/otherwise. Expect higher mortality on SW aspect; lower on NE aspect.	SW aspect	100%	0%
		NE aspect	18%	82%
		Other	58%	42%
Contagion	Douglas-fir mortality presence/absence from 1-ac subplot, outside the variable radius plot. Nearby DF mortality could serve as a contagion for any mortality observed in the variable radius plot.	Present	74%	26%
		Absent	23%	77%
Score	Risk score (SCORE), based on QAGA, HLI, CWD, EDGE, RIDGE, SW, NE, CONTAGION (see figure 4 for details). Low risk <0, Moderate risk 0–1, High risk 2–5, Very high risk 6–7	Low	0%	100%
		Moderate	45%	55%
		High	77%	23%
		Very high	88%	12%
Crown	Plot mean crown loss rating, 0–4s. 0 = 0% recent crown loss, 1 = 0–25% loss, 2 = 25–50% loss, 3 = 50–75% loss, 4 = 75–100% loss.			

site. These were defined as contiguous patches of dead tree crowns and ranged in size from a few trees to more than an acre in size. Mortality patches were mapped from high-resolution 2018 aerial imagery and the locations field-verified to ensure that the patches consisted primarily of DF. Within each mortality patch we installed one to five plots along a transect aligned with the longest patch dimension. We averaged or used the majority value for the plots within each patch, so that there was one plot per mortality patch in the final dataset. We removed six grid plots that fell within 50 m of mortality patch plots from further consideration. The final dataset included ninety-six plots (seventy-three grid and twenty-three mortality patch plots).

Prior field observation suggested that DF mortality was common along stand edges, perhaps due to elevated temperatures and moisture stress. We used a custom geographic information system tool in ArcMap to delineate stand edges and then calculated the distance from edge to plot center. The tool created a binary raster of stand edges based on tree height data from lidar, using a tree height break value of 22.9 m (75 feet). Mean values in a neighborhood close to 0 indicated “not trees”, values close to 1 indicated trees, and intermediate values indicate a mixture of trees and “not trees,” that is, edge. Field testing indicated the tool worked well for delineating hard edges, for example, taller trees next to an opening.

We calculated the initial stand density for each plot, defined as the plot mean basal area of live, dead, and dying trees of all species. This variable was used as an approximation of stand density and competition prior to mortality to test the hypothesis that higher levels of competition were associated with greater mortality.

Data Analysis

To explore the relationships between stand-scale topographic, site factors, and DF mortality, we used logistic regression and general linear model approaches, which focused on two dependent variables, plot mortality status and plot mortality intensity. Plot mortality status was a measure of the likelihood of mortality at a given point and used a binary variable in which any plot with at least 20 ft²/ac of dead and dying DF was assigned a value of 1, and all other plots were assigned a value of 0. Plot mortality intensity was the proportion of DF basal area in the plot that was dead or dying. All statistical analyses were completed in the Statgraphics 19 (Statgraphics Centurion 19 2020) statistical package. We initially compared the percentage of plots with and without DF mortality for each environmental and stand variable. Continuous variables were binned based on breakpoints seen in the data to highlight differences in plot mortality status associated with higher and lower levels of the variable (Table 1). Next, each variable was considered individually as a potential predictor of plot mortality status and plot mortality intensity, using logistic regression for the former and a general linear models procedure for the latter. Because a number of the variables were highly correlated (e.g., heat load index and climatic water deficit), we decided to integrate several of the individual categorical and continuous variables into a single continuous variable, risk score. This was done subjectively by including variables that were statistically significant predictors in the univariate analysis or that we suspected were associated with mortality based on prior field observations, or both. Point values used with the variables were assigned subjectively based on the

strength of the statistical associations with mortality and field observations (figure 4, Table 1).

We used forward stepwise logistic regression to examine the relationship between the set of potential predictor variables and plot mortality status. Crown loss rating was not included in this analysis because of the smaller sample size obtained when using this variable ($n = 45$ instead of $n = 96$) and because it was only marginally important in the univariate analysis. This analysis was first completed using all the variables except risk score and then with the same variable set plus risk score. We then used stepwise forward multiple regression to assess the relationship between the predictor variables and plot mortality intensity, first without crown loss rating and then with this variable.

Investigation of Mortality Agents in Felled Trees

Our analysis relied heavily on ADS data and the assumption that much of the recent mortality of DF in the study area is caused by or associated with the FB. We were unable to test this assumption in our field plots because it was difficult to determine the causal agent in dead trees due to sapwood decay or extensive gallery development and wood boring by secondary beetles. However, we were able to fell and closely examine eighteen dying and declining DF in areas of recent and ongoing DF mortality in close proximity to three of our study sites. Each site had one or more FB-killed or attacked tree within 100 m based on the reliable diagnostic of woodpecker bark “shaving”. Dying and declining DF in this investigation had one or more of the following signs and symptoms: severe crown thinning or dieback, severe chlorosis, branchlet flagging, major branch dieback, dead tops, and woodpecker activity. The DBH ranged from 6 inches to 27 inches. Each of the felled trees was closely examined by a team of experienced forest entomologists and pathologists for signs, symptoms, and direct observations of insects and diseases suspected to have caused or contributed to the observed declines. Although limited and qualitative in scope, this investigation helps contextualize the observed DF mortality that has been attributed to the FB.

Results

ADS Data, Climate, and Vegetation

For the 1975–2019 period, ADS estimated cumulative mortality associated with the FB was nearly a half million trees, with more trees dying in the 4-year period from 2015 to 2019 than in the previous four decades. During this same time period, mortality associated with the DFB was comparatively minor, according to ADS data (figure 5).

The intensity of mortality as measured by the number of FB-killed trees per km² was strongly associated with 1990–2020 average climate (figure 6). Higher mortality levels were associated with lower annual precipitation, higher mean annual climatic water deficit, higher maximum summer temperature, and higher summer maximum vapor pressure deficit. Grid cells with more than 100 trees killed/km² accounted for only 4% of the total area but 67% of the total trees killed, and these cells had lower annual precipitation, higher mean climatic water deficit, and higher maximum summer vapor pressure deficit (VPD) than cells with lower mortality levels. Conversely, grid cells with no recorded FB mortality had the highest precipitation, lowest climatic water deficit, and lowest summer maximum VPD.

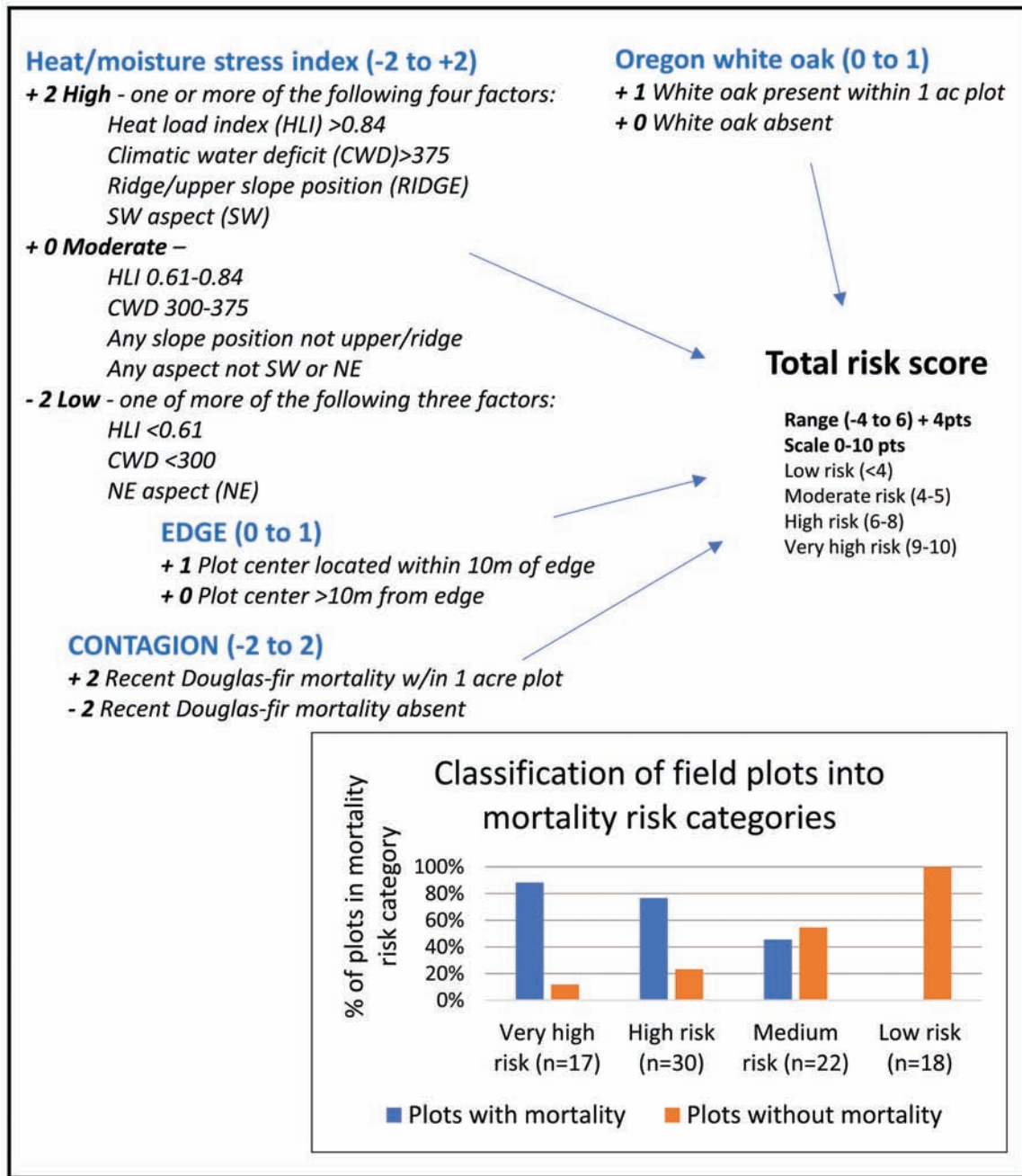


Figure 4. Calculation of site-scale Douglas-fir mortality risk based on key risk factors identified in the Oregon study site data. Risk levels refer to the likelihood of encountering Douglas-fir mortality and of mortality intensification at a given point. Bar chart shows classification of study site data into each risk score category based on this scoring rubric and percent of all study site plots falling into each category.

Mean elevation per grid cell was similar across mortality levels.

We observed that FB mortality generally occurred when 2-year growing season SPI and growing season PDSI were negative, that is, during periods of drought (figure 7). The FB mortality increased substantially in 2015, a year when these drought indices were negative but not unusually so compared with the recent past. However, in 2015, the 2-year running average of minimum summer temperatures was elevated.

In the analysis comparing locations of recent FB mortality (2000–2019) with historic vegetation, we found that 50% of the mapped mortality acreage and 47% of the trees killed

were in locations mapped as ponderosa pine or oak types in the 1936 map. This suggests that about half of contemporary DF mortality has occurred in areas where it was not the dominant species historically but has encroached on or increased in abundance due to fire exclusion.

Field Data

The study sites were broadly similar in elevation, climatic water deficit, and the percentage of plots with DF mortality (Table 2) but differed in their amount of live and dead and dying basal area. Across all sites, DF was the dominant species, accounting for 65% of the live basal area and 97%

of the basal area of dead and dying trees, with dead trees accounting for >90% of this total (Table 2). Virtually all of dead trees were decay class 1 snags and most appeared to have died within the past 10 or fewer years based on fine branch and bark retention and the extent of sapwood decay.

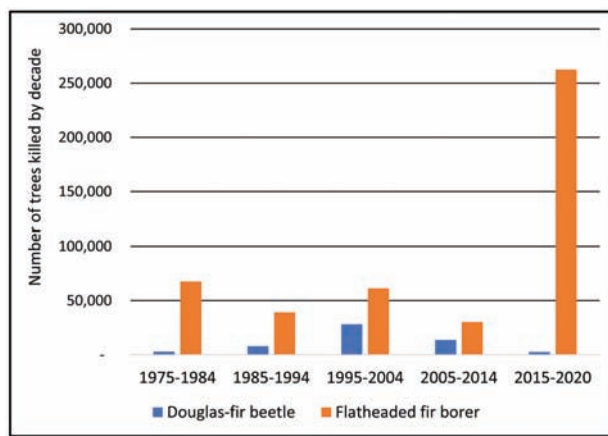


Figure 5. Number of trees killed by Douglas-fir beetle (DF) and flatheaded fir borer (FB) between 1975 and 2020, based on Aerial Detection Survey data. More trees were killed by the FB in 2015–2019 than in the previous four decades. Mortality associated with the DF beetle was comparatively minor.

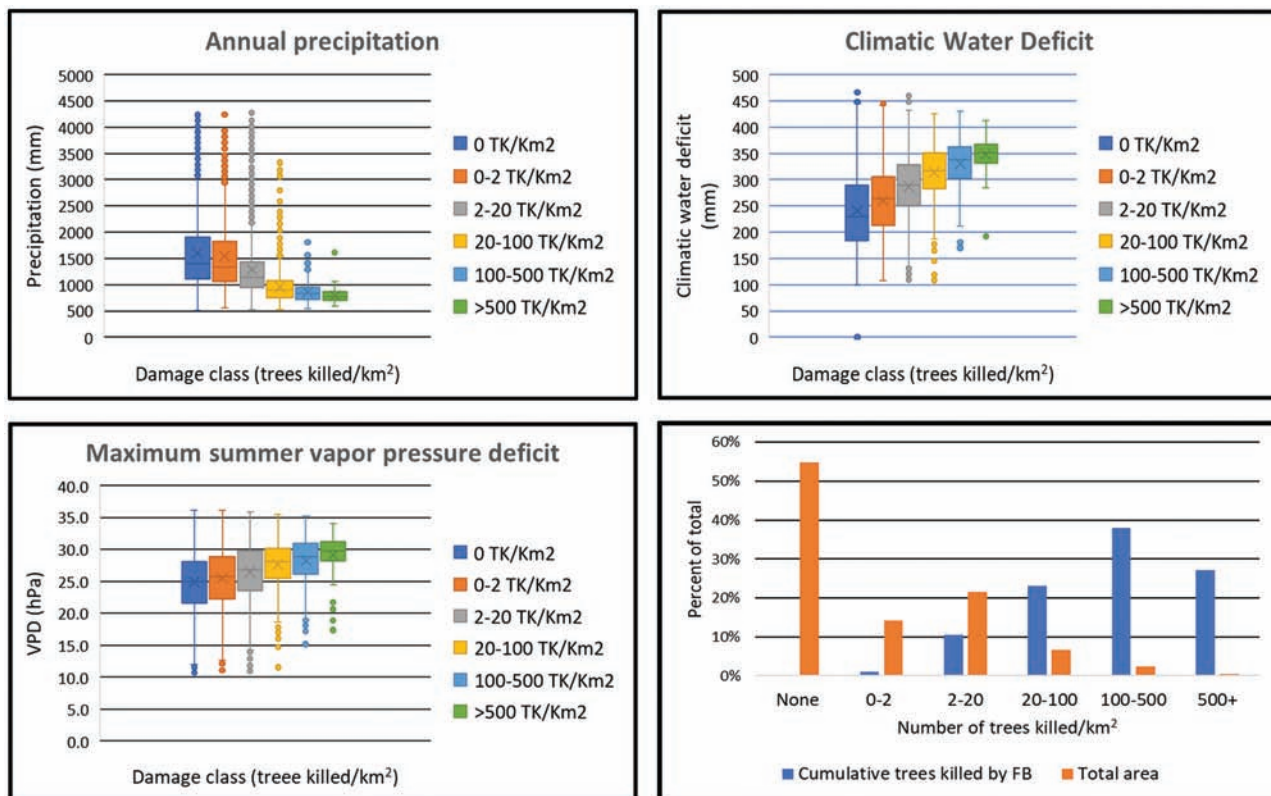


Figure 6. Box plots for number of trees killed per square kilometer in relation to climate variables. Number of trees killed (TK)/km² (1 km square grid cell) is derived from Aerial Detection Survey data, cumulative for 2000–2019, for Douglas-fir mortality in the study area attributed to the flatheaded fir borer (FB). Climate variables are means for grid cells based on the 1990–2020 “normals” from PRISM for annual precipitation, climatic water deficit, and maximum summer vapor pressure deficit. Higher levels of FB mortality are associated with lower mean precipitation, higher mean climatic water deficit (CWD), and higher maximum vapor pressure deficit (VPD, mean of June–August). Mean elevation is similar across levels of mortality (not shown). Bar graph compares percent of total cumulative trees killed with each damage class to percent of total area represented by damage class. About two-thirds of the cumulative mortality occurred within the 4% of the grid cells that represent locations with the hottest, driest climate.

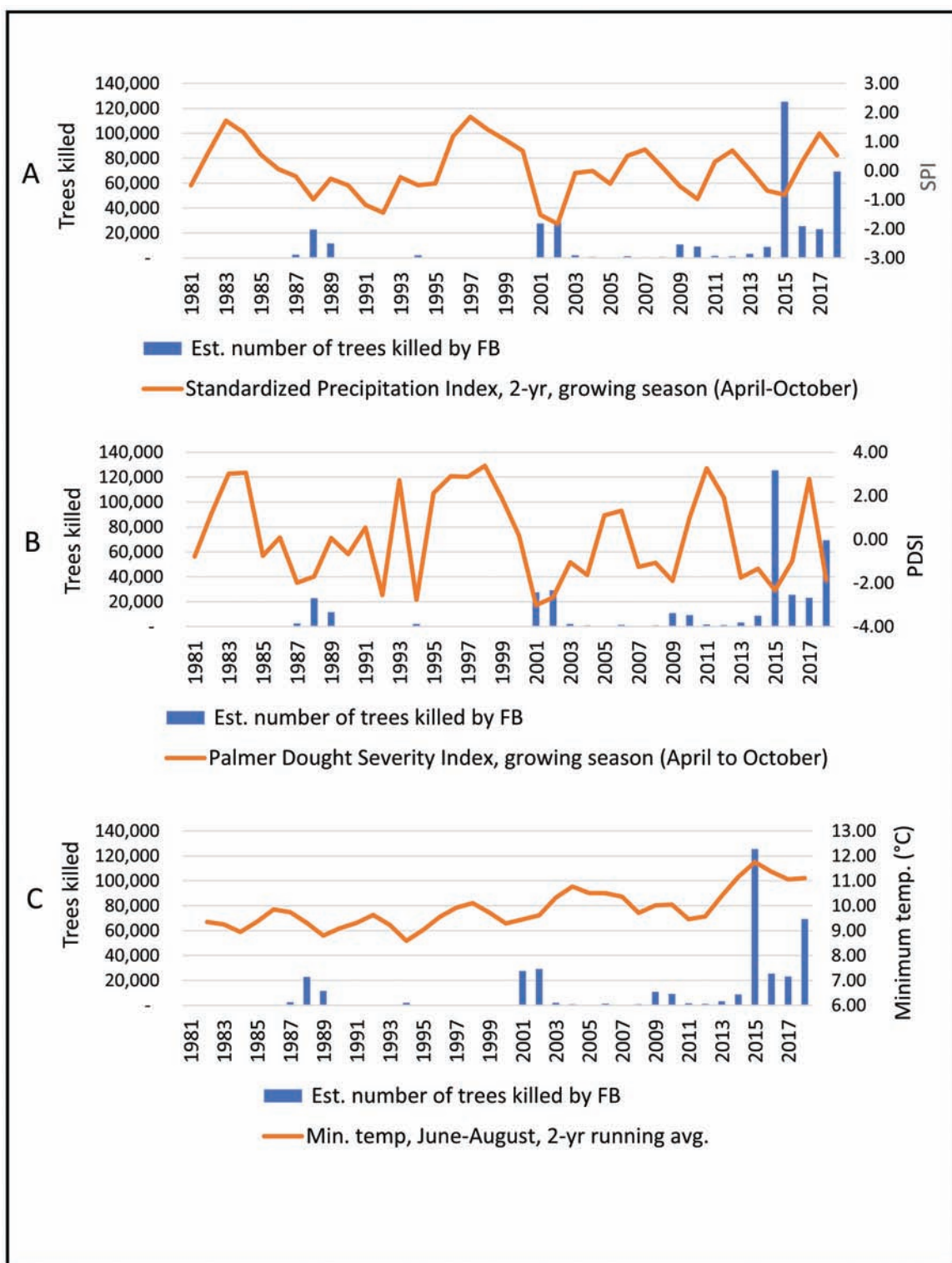


Figure 7. Relationship of annual flatheaded fir borer (FB) mortality, 1981–2018 in Klamath Mountains ecoregion, Oregon, and A), 2-year growing season Standardized Precipitation Index (SPI); B), growing season Palmer Drought Severity index (PDSI); and C), 2-year running average of summer minimum temperatures, based on mean values of gridded data for each variable within the analysis area. Douglas-fir mapped by Aerial Detection Survey as FB were attributed as killed the prior growing season. Years of higher FB mortality are associated negative SPI and PDSI. The 2015–2018 period did not feature an unusually severe precipitation drought, but summer minimum temperatures were elevated compared to the recent past.

variable effectively integrated information from several of the other variables, with slightly improved overall performance (explained deviance of 28% versus 25% for the initial model

without risk score). There was a positive linear relationship between risk and the percentage of plots with mortality (figure 4, bar graph). The only significant predictor of plot

Table 2. Characteristics of study sites and field plots. Study sites were similar in elevation, climatic water deficit and percentage of plots with mortality, but differed in live and dead/dying basal area. Across all sites, DF mortality was widely distributed, with approximately half of the grid plots containing at least one dead/dying DF. About one third of the total DF basal area across all plots was dead/dying.

Study site	Acres	Number of plots	Mean elev. (m)	Climatic water deficit (mm)	Percent of plots with mortality	Mean live BA, all species	DF BA, live	DF BA, dead & dying
Canyon-ville	333	13	386	305	62	138	73	55
Ashland	196	20	777	359	60	97	56	19
Collins	157	24	621	346	67	81	35	42
Pilot Joe	673	39	561	335	49	111	81	35
Grid plots	-	73	607	337	44	123	80	20
Mortality patch plots	-	23	591	344	100	47	10	88
All plots	-	96	603	338	57	105	63	36

Table 3. Results of statistical analysis of field plot data. Univariate analysis of predictor variables for plot mortality status and percent mortality. The analysis with plot mortality status used logistic regression; the analysis for percent mortality used a general linear models procedure. Significant ($P < 0.05$) predictor variables were the same for both response variables.

Predictor variable	Mean of plots		Plot mortality status (1, 0)		Percent mortality (0-100%)	
	With mortality	No mortality	P-value	% Deviance explained	P-value	R-squared
Climatic water deficit (CWD)	348.4	325.4	0.001	6%	0.008	10%
Crown loss rating (CROWN) ¹	1.16	0.64	0.030	1%	0.002	18%
Distance to edge (EDGE)	37.1	69.2	0.010	2%	0.010	6%
Heat load index (HLI)	0.78	0.65	0.001	6%	0.004	8%
Initial BA (BA)	140.3	142.9	0.830	0%	0.620	0%
Risk score (SCORE)	7.25	3.66	0.000	28%	0.000	37%
Slope (SLOPE)	36.6	42.2	0.140	0%	0.167	1%
Topographic position index (TPI)	1.1	-24.1	0.230	0%	0.190	0%
Nearby DF mortality (CONTAGION)			0.001	15%	0.000	22%
NE aspect (NE)			0.005	3%	0.002	9%
SW aspect (SW)			0.002	4%	0.008	6%
Ridge/upper slope position (RIDGE)			0.060	0%	0.220	0%
White oak present (QUGA)			0.001	2%	0.001	11%

¹ Based on $n = 45$ observations; all others based on 96 observations. Adjusted R-squared = 46.6%.

Table 4. Results of logistic regression, forward stepwise procedure for predictor variables and plot mortality status. Risk score was the only selected variable.

Parameter	Estimated regression model (maximum likelihood)			Analysis of deviance			
	Estimate	Standard error	Estimated odds ratio	Source	Deviance	DF	P-value
Constant	-3.14	0.76		Model	41.7	1	0.00
Risk score	0.61	0.12	1.83	Residual	89.3	94	0.62
				Total (corr.)	131.0	95	

Adjusted percentage of deviance explained by model = 28.8

mortality intensity in the stepwise forward regression model without crown loss ($n = 96$) was risk score, which explained 37% of the variation (data not shown). When crown loss was added ($n = 45$), the selected model included risk score, crown loss, and SW aspect (Table 5), which explained about half of the variation in plot mortality intensity.

Mortality Agents in Felled Trees

Flatheaded fir borer galleries or larvae were found on 43% of the sampled trees (Figure 8). We also noted pitch pockets in the growth rings on stumps of several of the felled trees, suggesting that the trees may have overcome previous FB attacks. We observed galleries and larvae of several species of secondary

Table 5. Results of multiple linear regression for predictor variables and percent mortality. Risk score, crown loss rating, and SW aspect were selected. This analysis used the forty-five observations for which crown loss data were available.

Parameter	Estimate	Std Error	T Statistic	P-value	Analysis of variance				
Constant	-0.10	0.05	-2.12	0.039	Source	Sum of squares	DF	Mean Square	F-Ratio
Crown loss rating	0.09	0.03	2.87	0.065	Model	1.03	3	0.34	13.79
Risk score	0.03	0.01	3.27	0.002	Residual	1.02	41	0.02	
Aspect-SW	0.28	0.01	2.85	0.007	Total (corr.)	2.05	44		

Adjusted R-squared = 46.6%

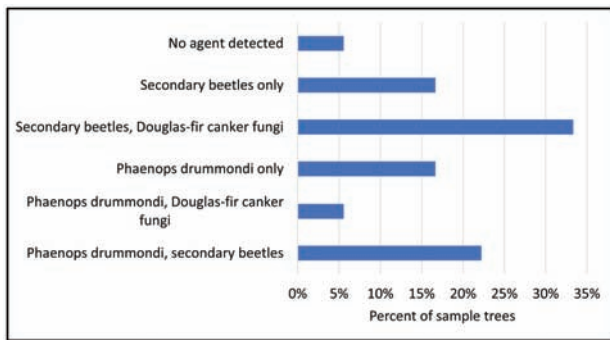


Figure 8. Results of investigation of nineteen declining and dying Douglas-fir trees conducted spring and fall 2021 for signs, symptoms, and direct observations of insects and diseases suspected to have caused or contributed to the observed decline. Chart shows percent of sample trees hosting agent types. Multiple agents were present in most declining trees, suggesting that a complex is responsible for the decline rather than *Phaenops drummondi* acting alone.

wood boring beetles in the *Buprestidae* and *Cerambycidae* families, as well as the bark beetles *Scolytus unispinosus* (Coleoptera: Curculionidae) and *Pseudohylesinus nebulosus* (Coleoptera: Curculionidae) in most of the trees. The DF canker fungi *Diaporthe lokoyae* or *Dermea boycei* were encountered in the branches or the upper boles of several trees. We found no evidence of root disease or Douglas-fir beetle (*Dendroctonus pseudotsugae*) on any of the sample trees.

Discussion

This study leveraged data from the ADS and field plots to examine the relationship between DF mortality and climate and environmental variables at the landscape and stand scales. Our results provide strong evidence for the hypothesized DF decline spiral (figure 2) in which DF trees growing on already water-stressed, marginal sites are further stressed by drought and are then exploited by the FB and other secondary biotic agents, resulting in decline and mortality. We did not explore the possible role of cavitation in DF decline, but we think this is likely to be an important factor given the relationships between drought and hydraulic failure that has been found in forest declines involving a wide range of species (Adams et al. 2017; McDowell et al. 2008).

At the landscape scale, FB mortality was observed across wide precipitation and elevation gradients, but the majority of the mortality was detected on the hottest, driest sites in and around the interior valleys (figure 3) at low to moderate elevations (400–1400 m). The number of DF trees killed per 1-km grid cell was associated with long-term (1990–2020)

averages for annual precipitation, annual CWD, and maximum summer VPD (figure 6), and these variables could be used to identify locations with higher and lower relative mortality risk. However, there was considerable noise in these data, making it difficult to determine absolute mortality risk in any given location.

At the stand scale, our results suggest that DF mortality is more likely to be encountered and to be more severe in locations with a high heat load index (e.g., southwest aspects), a high climatic water deficit, and in proximity to recent DF mortality related to the FB. They also suggest that DF mortality may be reduced in more topographically favorable locations where heat load and water deficit are lower, such as northeast aspects. This is consistent with the landscape-scale data showing higher DF mortality levels on hotter, drier sites and lower mortality on more mesic sites. Other studies in a range of western forest types have found similar relationships between topo-edaphic variability and tree mortality (e.g., Bost et al. 2019; Powers et al. 2009; Worrall et al. 2008). Our results also provided some evidence for an association between DF mortality and white oak presence and proximity to stand edges.

The ADS and weather data suggest that FB mortality increases sharply during and immediately after a major drought. Until the last decade, these increases were generally short-lived, of 1 to 3 years. Since 2009, however, there has been measurable FB mortality in the study area each year, with a dramatic increase observed in and after 2015. Precipitation drought (SPI) during the 2015–2018 period was not unusually intense or long-lasting, but minimum and maximum summer temperatures were elevated. This suggests that hotter drought (Hammond et al. 2022), a combination of higher temperatures and reduced precipitation, is associated with the increased FB mortality.

Our data comparing recent DF mortality and dominant vegetation circa 1936 suggest that much of the mortality occurred on sites where DF was not the dominant species in the past. Although we lacked data on changes within vegetation types since 1936, we suspect that fire exclusion has also resulted in increased densities of DF in areas mapped as “Douglas fir” in the historic vegetation map. These conclusions are consistent with local and regional data showing that fire was historically much more frequent in the interior portions of the ecoregion and that stand densities have increased as a result of fire exclusion. Changes in species composition in the ecoregion following fire exclusion are less well documented but are indicative of increased proportions of DF (Hosten et al. 2007; Knight et al. 2020; Leonzo and Keyes 2010) and DF encroachment in Oregon white oak woodlands has been widely observed (Barnhart et al. 1996; Cocking et al. 2014; Schriver et al. 2018).

As expected, plots were more likely to have DF mortality if there were dead and dying DF trees found outside the variable radius plot but nearby. This relationship is consistent with a contagion effect, in which the FB and other pests spread from infested trees to trees growing in close proximity. However, it could also be accounted for by the similar environments the plot trees and nearby infested trees were growing in. Regardless, proximity to nearby mortality serves as a useful predictor of the likelihood of DF mortality and mortality intensification at a given point in sites similar to those in this study.

Stand edges experience higher evaporative demand than stand interiors due to greater exposure to solar radiation and wind, which might then increase tree stress levels and subsequent vulnerability to pests or abiotic damage (Burras et al. 2018). Higher heat loads on stand edges might also increase tree respiration rates and potentially reduce carbon storage, contributing to higher vulnerability to mortality. In addition, edges may reflect a transition to shallow or rocky soils where moisture availability is reduced. Prior field observation in southwestern Oregon suggested that DF mortality was more common on stand edges and our plot data provided some support for this observation, but the relationship between proximity to edge and the response variables was not particularly strong.

There is a large body of research showing that high stand densities are associated with reduced tree vigor and subsequent increases in tree mortality (e.g., Bradford and Bell 2017; Furniss et al. 2022; Gleason et al. 2017). However, we did not see a clear relationship between stand density and either the likelihood or intensity of DF mortality in our plot data. This may suggest the DF decline and mortality in the biophysical settings considered in this study is not strongly influenced by inter-tree competition, or that any competitive effects were masked by variation in site productivity and carrying capacity.

Our team of experienced forest entomologists and pathologists examined felled DF that were dying or declining and in areas of ongoing DF mortality that had been attributed to the FB. There was evidence of the FB in about half of the sample trees, but nearly all of the trees hosted multiple agents including some combination of wood borers, secondary bark beetles, and canker diseases. This finding suggests that a complex may be responsible for DF decline and mortality in the ecoregion, rather than *Phaenops drummondi* acting alone. We suspect that many of the declining and dying DF may also be hydraulically compromised due to embolisms resulting from cavitation, but an investigation of this possibility was beyond the scope of this study.

An interesting observation was the relative lack of recently mapped mortality associated with the DF beetle (DFB, figure 5), which is thought to be a major mortality agent of DF regionally (Goheen and Wilhite 2021). In the Klamath ecoregion the ADS reports low mortality levels from the DF beetle since 1975 when local experts decided to code FB in the Klamath based on ground sampling of dead DF that yielded no DFB, and we did not observe the DFB on our plots or felled trees. In western Oregon, DFB-caused mortality is associated with wind-throw, drought, root disease, and wildfire (Goheen and Willhite 2021; Lowrey 2022 personal observation), but Powers et al. (1999) also found that landscape-scale mortality from the DFB was associated with drier sites and more mature and old-growth vegetation. The absence of recent large-scale DFB outbreaks in the Klamath ecoregion could be

explained by environmental conditions or poor host quality (carbohydrate status) resulting from the type of stress-related decline spiral seen in this study that is in some way inadequate for DFB development.

Management Implications

Our results inform assessments of DF mortality risk in the Klamath Mountains ecoregion. At the landscape scale, areas in the ecoregion with less than 1,000 mm (39 in.) annual precipitation or with a CWD greater than 300 mm (12 in.) have accounted for the great majority of mortality in the last two decades and this is likely to hold true in the near future. Although mortality has occurred along a large elevational gradient, most of the mortality has occurred in the 400 m to 1,000 m (1,312–4,593 ft) elevation band where this band overlaps with zones of low precipitation and high CWD. These higher risk zones account for only about 10% of the forest area in the ecoregion and are concentrated on the forested fringes of the interior valleys, often on private land.

Long term average CWD in particular seems promising as a risk assessment tool. Our data show that it is linearly associated with DF mortality levels in the ecoregion, conceptually it integrates several variables associated with moisture stress, and it correlates well with existing vegetation (Stephenson 1990). Young et al. (2017) also found a strong relationship between long-term average CWD and tree mortality in the Sierra Nevada following the extreme drought of 2012–2015. Predictions of future CWD can be used to assess future DF viability in the Klamath ecoregion. Although we are not aware of studies evaluating DF presence and cover in relation to CWD, local field observations suggest that DF is seldom found when the average long-term CWD exceeds about 400 mm (16 in.). Projected CWD in 2055 (Cansler et al. 2022) under an Representative Concentration Pathway (RCP) 8.5 scenario indicates that many areas that are currently below this threshold will exceed it, putting many DF at greater risk (figure 9).

At the stand scale, our risk score can be used to predict the likelihood and intensity of mortality based on topographic and site factors in locations similar to our study sites where there has already been significant but variable mortality. However, there is considerable variability in mortality levels within and across sites that is not explained or predicted by the environmental variables that make up the risk score. For example, some DF mortality is seen on north slopes, in riparian zones, and in the interiors of stands. We expect these trends to continue as hotter droughts continue and intensify. Specifically, future mortality is likely on the most climatically marginal sites for DF, regardless of topo-edaphic variation, and sites may need to be recategorized for risk and hazard as climates shift.

Although DF mortality is likely to increase, we caution against concluding that all DF trees in high-risk locations will die in the near future and should be “written off.” The DF patches occupying steep northeast aspects, for example, are somewhat buffered from moisture stress and may serve as refugia. We have also observed, within patches of extensive DF mortality, some individual DF trees that have persisted and appear vigorous based on traditional crown metrics, for example, crown ratio, color, and foliage density. The reasons for this persistence and implications for future DF viability on such sites merit further study.

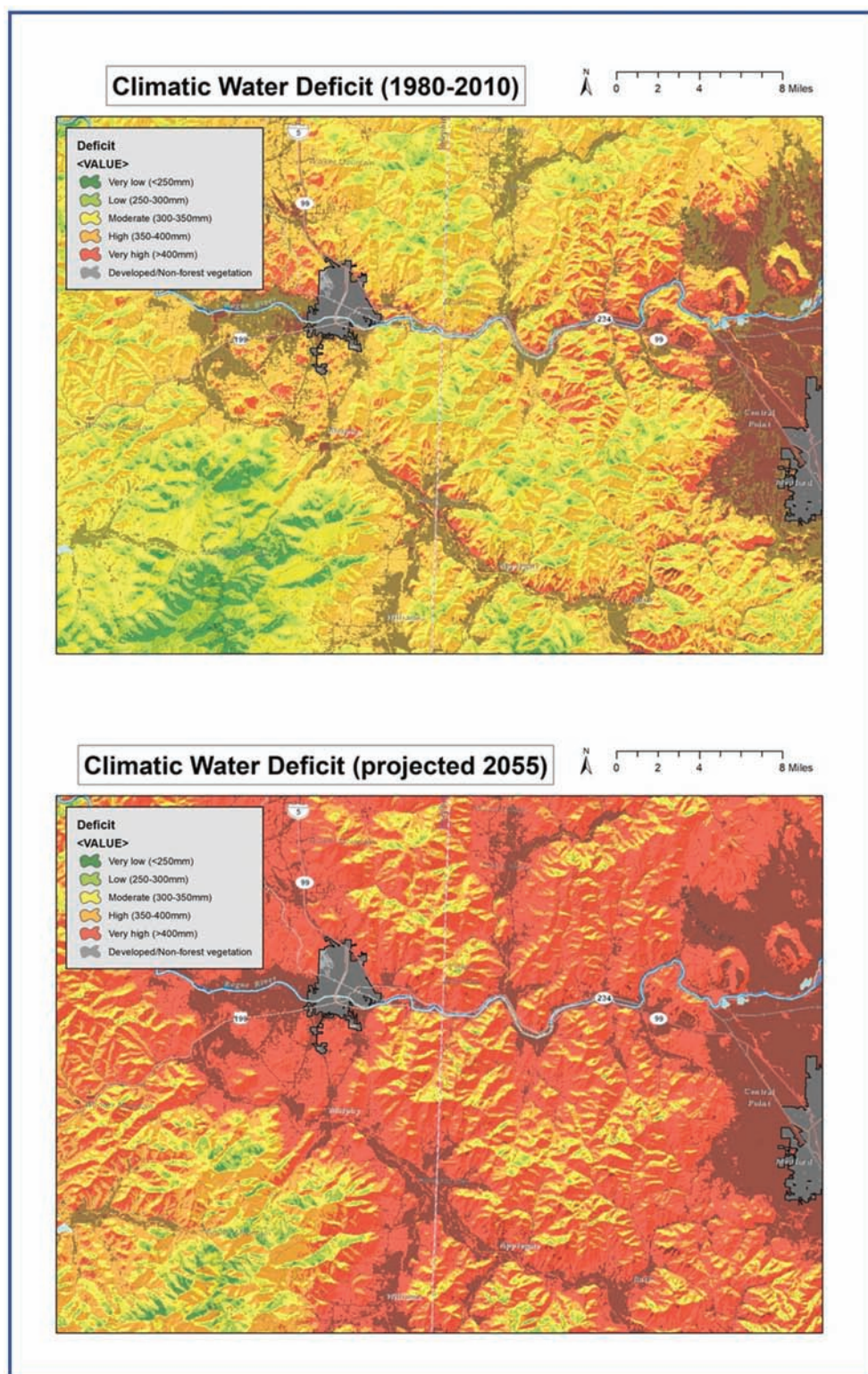


Figure 9. Recent (1980–2010) and projected (2055) climatic water deficit (CWD) for a portion of the Klamath ecoregion, Oregon. Projected CWD is based on a conservative Representative Concentration Pathway 8.5 scenario. Data suggest than Douglas-fir mortality risk is significantly elevated above a CWD of 350 and few DF are found above a CWD of 400. Under the projected CWD, most lower elevation sites in interior SW Oregon would be inhospitable for Douglas-fir.

A key consideration in management of DF in the Klamath ecoregion is the ability of a site to support DF now and in the future. On more favorable sites, thinning to retain the most vigorous DF may increase their resistance to the suite

of pests and abiotic damage associated with DF decline, at least in the short to medium term. On harsher sites, thinning might instead focus on aggressively removing declining DF and moving the stand to a higher proportion of pines, oaks,

and other more drought and fire-resistant species. This will also help mitigate fuels buildups associated with DF mortality in these areas. More research is needed to clarify the potential of thinning to improve DF resistance and resilience on marginal sites.

Conclusions

Mortality of DF in the Klamath Mountains ecoregion is a result of a complex interaction of biotic and abiotic factors and is not caused solely by one specific biological agent or environmental factor. The Manion decline spiral captures the dynamics of these interactions as a causal chain of predisposing (dry sites at low elevations where DF was historically rare and where fire suppression has influenced forest structure and composition), inciting (hot drought), and contributing (cavitation, FB, other bark beetles and canker diseases) factors that work together to cause tree mortality. We developed a risk assessment tool that allows managers to identify current and future sites susceptible to mortality by integrating these factors.

Acknowledgements

For assistance with the field investigation of mortality agents in felled trees, we thank Don Goheen, Barb Lachenbruch, Marty Main, Bill Schaupp, Holly Kearns, Kristen Chadwick, and Beth Wilhite. The Medford District Bureau of Land Management provided and felled the trees for this investigation. For assistance with data collection, we thank Gary Clarida, Clem Stockard, Kara Baylog, Chris VanNess, and students at Logos school in Medford, Oregon. Thanks to Karen Wolken for assistance with data analysis, and to Marty Main, Bill Schaupp, and Don Goheen for ongoing collaboration in investigating the Douglas-fir mortality issue.

Literature Cited

Adams, H.D., M.J.B. Zeppel, W.R.L. Anderegg, H. Hartmann, S.M. Landhäuser, D.T. Tissue, T.E. Huxman, et al. 2017. "A Multi-Species Synthesis of Physiological Mechanisms in Drought-Induced Tree Mortality." *Nature Ecology and Evolution* 1 (9): 1285–91. doi:[10.1038/s41559-017-0248-x](https://doi.org/10.1038/s41559-017-0248-x).

Agne, M.C., P.A. Beedlow, D.C. Shaw, D.R. Woodruff, E.H. Lee, S.P. Cline, and R.L. Comeleo. 2018. "Interactions of Predominant Insects and Diseases with Climate Change in Douglas-fir Forests of Western Oregon and Washington, U.S.A." *Forest Ecology and Management* 409: 317–32. doi:[10.1016/j.foreco.2017.11.004](https://doi.org/10.1016/j.foreco.2017.11.004).

Barnhart, S.J., J.R. McBride, and P. Warner. 1996. "Invasion of Northern Oak Woodlands by *Psuedotsuga menziesii* (Mirb.) Franco in the Sonoma Mountains of California." *Madroño* 43 (1): 2845. <https://www.jstor.org/stable/41425115>.

Bost, D.S., M.J. Reilly, E.S. Jules, M.H. DeSiervo, Z. Yang, and R.J. Butz. 2019. "Assessing Spatial and Temporal Patterns of Canopy Decline Across a Diverse Montane Landscape in the Klamath Mountains, CA, USA Using a 30-Year Landsat Time Series." *Landscape Ecology* 34 (11): 2599–14. doi:[10.1007/s10980-019-00907-7](https://doi.org/10.1007/s10980-019-00907-7).

Bradford, J.B., and D.M. Bell. 2017. "A Window of Opportunity for Climate-Change Adaptation: Easing Tree Mortality by Reducing Forest Basal Area". *Frontiers in Ecology and the Environment* 15 (1): 11–7. doi:[10.1002/fee.1445](https://doi.org/10.1002/fee.1445).

Buhl, C., Navarro, S., Norlander, D., Williams, W., Heath, Z., Ripley, K., Schroeter, R., and Smith, B. 2017. *Forest Health Highlights in Oregon* 2017. USDA Forest Service and Oregon Department of Forestry. https://www.fs.usda.gov/Internet/FSE_DOCUMENTS/fsepr595221.pdf. Date accessed 1 February 2022.

Buras, A., C. Schunk, C. Zeitrg, C. Herrmann, L. Kaiser, H. Lemme, C. Straub, et al. 2018. "Are Scots Pine Forest Edges Particularly Prone to Drought-Induced Mortality?". *Environmental Research Letters* 13: 025001. doi:[10.1088/1748-9326/aa0b4](https://doi.org/10.1088/1748-9326/aa0b4).

Buttrick, S., K. Popper, M. Schindel, B. McRae, B. Unnasch, A. Jones, and J. Platt. 2015. *Conserving Nature's Stage: Identifying Resilient Terrestrial Landscapes in the Pacific Northwest*, 104. Portland, OR: The Nature Conservancy. <http://nature.ly/resilienceNW>. Date accessed 1 December 2021.

Cansler, C.A., V.R. Kane, P.F. Hessburg, J.T. Kane, S.M.A. Jeronimo, J.A. Lutz, N.A. Povak, et al. 2022. "Previous Wildfires and Management Treatments Moderate Subsequent Fire Severity". *Forest Ecology and Management* 504: 119764. doi:[10.1016/j.foreco.2021.119764](https://doi.org/10.1016/j.foreco.2021.119764).

Climate Toolbox. <https://climatetoolbox.org/>. Date accessed 1 February 2022.

Cocking, M.I., J. Morgan Varner, and E.A. Engber. 2014. *Conifer Encroachment in California Oak Woodlands*. USDA Forest Service General Technical Report PSW-GTR-251. https://www.fs.usda.gov/psw/publications/documents/psw_gtr251/psw_gtr251_505.pdf. Date accessed 1 March 2022.

Coleman, T.W., A.D. Graves, Z. Heath, R.W. Flowers, R.P. Hanavan, D.R. Cluck, and D. Ryerson. 2018. "Accuracy of Aerial Detection Surveys for Mapping Insect and Disease Disturbances in the United States". *Forest Ecology and Management* 430: 321–36. doi:[10.1016/j.foreco.2018.08.020](https://doi.org/10.1016/j.foreco.2018.08.020).

Franklin, J.F., and C.T. Dyrness. 1988. *Natural Vegetation of Oregon and Washington*, 427. Corvallis, OR: Oregon State University Press.

Furniss, R.L., and V.M. Carolin. 1977. *Western Forest Insects*. Miscellaneous Publication No. 1339. Washington, DC: USDA Forest Service.

Furniss, T.J., A.J. Das, P.J. van Mantgem, N.L. Stephenson, and J.A. Lutz. 2022. "Crowding, Climate, and the Case for Social Distancing Among Trees". *Ecological Applications* 32 (2): e2507. doi:[10.1002/ecs2.2507](https://doi.org/10.1002/ecs2.2507).

Gibson, K. 2010. *Management Guide for Flatheaded Fir Borers*. US Forest Service, Forest Health Protection. https://www.fs.usda.gov/Internet/FSE_DOCUMENTS/stelprdb5187437.pdf. Date accessed 15 March 2022.

Gleason, K.E., J.B. Bradford, A. Bottero, A.W. D'Amato, S. Fraver, B.J. Palik, M.A. Battaglia, et al. 2017. "Competition Amplifies Drought Stress in Forests Across Broad Climatic and Compositional Gradients". *Ecosphere* 8 (7): e01849. doi:[10.1002/ecs2.1849](https://doi.org/10.1002/ecs2.1849).

Goheen, E.M., and E.A. Wilhite. 2021. *Field Guide to Common Diseases and Insect Pests of Oregon and Washington Conifers*, 325. Rev. ed. R65-FHP-RO-2021-01. Portland, OR: USDA Forest Service, Pacific Northwest Region.

Halofsky, J.E., D.L. Peterson, and R.A. Gravenmier. 2022. *Climate Change Vulnerability and Adaptation in Southwest Oregon*, 445. Gen. Tech. Rep. PNW-GTR-995. Portland, OR: USDA Forest Service, Pacific Northwest Research Station. <https://www.fs.usda.gov/pnw/pubs/pnw-gtr995.pdf>. Date accessed 15 September 2022.

Hessburg, P.F., C.L. Miller, S.A. Parks, N.A. Povak, A.H. Taylor, P.E. Higuera, et al. 2019. "Climate, Environment, and Disturbance History Govern Resilience of Western North American Forests". *Frontiers in Ecology and Evolution* 7: 239. doi:[10.3389/fevo.2019.00239](https://doi.org/10.3389/fevo.2019.00239).

Hammond, W.M., A.P. Williams, J.T. Abatzoglou, H.D. Adams, T. Klein, R. López, C. Sáenz-Romero, et al. 2022. "Global Field Observations of Tree Die-off Reveal Hotter-Drought Fingerprint for Earth's Forests". *Nature Communications* 13 (1): 1761. doi:[10.1038/s41467-022-29289-2](https://doi.org/10.1038/s41467-022-29289-2).

Hosten, P., Hickman, O.E., & Lang, F. 2007. *150 Years of Vegetation Change in the Grasslands, Shrublands, and Woodlands of Southwest Oregon*. Medford, OR: U.S. Bureau of Land Management.

<http://soda.sou.edu/bioregion.html>. Date accessed 1 December 2021.

Hoyleman, Z.H., K.G. Jencso, J. Hu, J.T. Martin, Z.A. Holden, C.A. Seielstad, and E.M. Rowell. 2018. "Hillslope Topography Mediates Spatial Patterns of Ecosystem Sensitivity to Climate." *Journal of Geophysical Research, Biogeosciences* 123 (2): 353–71. doi:10.1002/2017JG004108.

Jenness, J. 2006. Topographic Position Index (tpi_jen.avx) extension for Arc-View 3.x, v. 1.2. Jenness Enterprises. <http://www.jennessent.com/arcview/tpi.htm>. Date accessed 1 October 2021.

Knight, C.A., C. Cogbill, M.D. Potts, J.A. Wanket, and J.J. Battles. 2020. "Settlement-era Forest Structure and Composition in the Klamath Mountains: Reconstructing a Historical Baseline". *Ecosphere* 11 (9): e03250. doi:10.1002/ecs2.3250.

Landscape Ecology Modeling Mapping and Analysis (LEMMA). 2014. <http://lemma.forestry.oregonstate.edu/data/>. Accessed 1 December 2021.

Leonzo, C.M., and C.R. Keyes. 2010. "Fire-Excluded Relict Forests in the Southeastern Klamath Mountains, California, USA". *Fire Ecology* 6 (3): 62–76. doi:10.4996/fireecology.0603062.

Malesky, D., T. Rhoades, C. Jorgensen, and G. McNamee. 2019. *Region 4 Cumulative Insect Impact Estimation 1991–2015*. USDA Forest Service, Intermountain Region R4-FHP-19-01, USDA Forest Service, Ogden, UT.

Manion, P.D. 1991. *Tree Disease Concepts*, 2nd ed, 402. Englewood Cliffs, NJ: Prentice-Hall.

McDowell, N., W.T. Pockman, C.D. Allen, D.D. Breshears, N. Cobb, T. Kolb, J. Plaut, et al. 2008. "Mechanisms of Plant Survival and Mortality During Drought: Why do Some Plants Survive While Others Succumb to Drought?" *New Phytologist* 178 (4): 719–39. doi:10.1111/j.1469-8137.2008.02436.x.

Metlen, K.L., C.N. Skinner, D.R. Olson, C. Nichols, and D. Borgias. 2018. "Regional and Local Controls on Historical Fire Regimes of Dry Forests and Woodlands in the Rogue River Basin, Oregon, USA". *Forest Ecology and Management* 430 (15): 43–58. doi:10.1016/j.foreco.2018.07.010.

National Center for Atmospheric Research. 2022. Climate Data Guide. <https://climatedataguide.ucar.edu/>. Date accessed 1 November 2021.

Oregon Department of Forestry. 2016. Flatheaded Fir Borer. Fact Sheet. 2. <http://tinyurl.com/odf-foresthealth>. Date accessed 1 December 2021.

Paz-Kagan, T., P.G. Brodrick, N.R. Vaughn, A.J. Das, N.L. Stephenson, K.R. Nydick, and G.P. Asner. 2017. "What Mediates Tree Mortality During Drought in the Southern Sierra Nevada?" *Ecological Applications* 27 (8): 2443–57. doi:10.1002/eaap.1620.

Powers, J.S., P. Sollins, M.E. Harmon, and J.A. Jones. 1999. "Plant-Pest Interactions in Time and Space: A Douglas-fir Bark Beetle Outbreak as a Case Study". *Landscape Ecology* 14: 105–20. doi:10.1023/A:1008017711917.

PRISM Climate Group, Oregon State University. <https://prism.oregonstate.edu>, data created 4 February 2014, Date accessed 16 December 2022.

Schaupp, Bill. 2017. "Increased Tree Mortality in the Applegate Adaptive Management Area". In *Applegate Valley Community Magazine*, 8. Spring 2017 and as a report on file at USDA Forest Service, Forest Health Protection. Medford, OR: Southwest Forest Insect and Disease Center.

Schaupp, W.C. Jr., and K.E. Strawn. 2016. "A 'primary' woodborer of low elevation Douglas-fir in southwest Oregon." Poster presented at the 2016 North American Forest Insect Work Conference, May 31 – June 6, Washington, D.C. https://www.cpe.vt.edu/nafiwc16/NAFIWC_2016_Proceedings.pdf. Date accessed 1 December 2022.

Schriver, M., R.L. Sherriff, J.M. Varner, L. Quinn-Davidson, and Y. Valachovic. 2018. "Age and stand structure of oak woodlands along a gradient of conifer encroachment in northwestern California". *Ecosphere* 9 (10):e02446. doi:10.1002/ecs2.2446.

Schulte, L., and D. Mladenoff. 2001. "The Original US Public Land Survey Records-Their Use and Limitations in Reconstructing Pre-settlement Vegetation". *Journal of Forestry* 99 (10): 5–10. doi:10.1093/jof/99.10.5.

Statgraphics Centurion 19. 2020. The Plains, VA: Statgraphics Technologies, Inc.

Stephenson, N.L. 1990. "Climatic Control of Vegetation Distribution: The Role of Water Balance". *The American Naturalist* 135 (5): 649–70. <https://www.jstor.org/stable/2462028>.

Tobalske, C. 2002. Historic Vegetation. Oregon Natural Heritage Program. 1:100,000. Shapefile. 60 MB. <https://inr.oregonstate.edu/hvmp/available-maps>. Date accessed 15 March 2022.

Vander Schaaf, D., M. Schindel, D. Borgias, C. Mayer, D. Tolman, G. Kittel, J. Kagan, et al. 2004. *Klamath Mountains Ecoregional Conservation Assessment*. Portland, OR: The Nature Conservancy. https://www.conservationgateway.org/ConservationPlanning/SettingPriorities/EcoregionalReports/Documents/Klamath_Mountains_Ecoregional_Assessment_report.pdf. Date accessed 15 September 2022.

Worrall, J.W., L. Egeland, T. Eager, R. Mask, E. Johnson, P. Kemp, and W. Shepperd. 2008. "Rapid Mortality of *Populus tremuloides* in Southwestern Colorado, USA". *Forest Ecology and Management* 255: 686–96. doi:10.1016/j.foreco.2007.09.071.

Young, D.J.N., J.T. Stevens, J.M. Earles, J. Moore, A. Ellis, A.L. Jirka, and A.M. Latimer. 2017. "Long-Term Climate and Competition Explain Forest Mortality Patterns Under Extreme Drought". *Ecology Letters* 20 (1): 78–86. doi:10.1111/ele.12711.